A Small-Angle Scattering Study of the Bulk Structure of a Symmetric Diblock Copolymer System

Christine Papadakis, Kristoffer Almdal, Kell Mortensen, Dorthe Posselt

J. Phys. II France **7** (1997) 1829–1854 DECEMBER **1997**, PAGE 1829

A Small-Angle Scattering Study of the Bulk Structure of a Symmetric Diblock Copolymer System

Christine M. Papadakis ([1,*]), Kristoffer Almdal ([2]),
Kell Mortensen ([2]) and Dorthe Posselt ([1])

([1]) IMFUFA (Institute of Mathematics and Physics), Roskilde University,
P.O. Box 260, DK-4000 Roskilde, Denmark
([2]) Condensed Matter Physics and Chemistry Department, Risø National Laboratory,
P.O. Box 49, DK-4000 Roskilde, Denmark

(Received 24 April 1997, received in final form 5 August 1997, accepted 1 September 1997)

PACS.61.41.+e – Polymers, elastomers, and plastics
PACS.64.60.Cn – Order-disorder transformations; statistical mechanics of model systems
PACS.61.12.Ex – Neutron scattering techniques (including small-angle scattering)

Abstract. — The bulk structure of a homologous series of symmetric polystyrene-polybutadiene (SB) diblock copolymers is investigated using small-angle X-ray and neutron scattering (SANS). The study focuses on the lamellar thickness, the lamellar correlation length and the concentration profile as a function of the chain length and the preparation method applied. The characteristic length, D, scales with the chain length, N, in the whole range studied, but with a clear change in scaling exponent near $\chi N = 29$, in accordance with theoretical predictions of a crossover from an Intermediate-Segregation Regime (ISR) to the Strong-Segregation Limit (SSL). In the ISR ($\chi N \simeq 5 - 29$), D is found to scale like $D \propto N^{0.83}$ and in the SSL ($\chi N > 29$) like $D \propto N^{0.61}$ The temperature dependence of the SANS spectra is studied for a low molar mass sample in an interval around the order-disorder transition temperature (T_{ODT}). The peak position is found to vary more strongly with temperature than expected for Gaussian chains. Only a weak discontinuity of the peak position at T_{ODT} is observed. In summary, the phase behavior of symmetric SB diblock copolymers in the bulk spans three regimes: the Gaussian regime in the region $\chi N < 5$, the ISR for $5 < \chi N < 29$ and the SSL for $\chi N > 29$.

1. Introduction

Diblock copolymers consist of two chemically distinct polymer blocks joined by a covalent bond. Their bulk phase behavior (*i.e.* without solvent present) can to a good approximation be described in terms of the volume fraction of one block, f, and the combined parameter χN, where χ denotes the Flory-Huggins segment-segment interaction parameter ($\chi \propto 1/T$, where T is the temperature) and N the chain length. A microphase-separated, ordered structure is formed for $\chi N > (\chi N)_{\mathrm{ODT}}$ [1]. ODT is short for order-disorder transition. Depending

(*) Author for correspondence (e-mail: Christine.Papadakis@risoe.dk)
Present address: Condensed Matter Physics and Chemistry Department, Risø National Laboratory, P.O. Box 49, DK-4000 Roskilde, Denmark

on f, different morphologies are formed in the ordered state, *e.g.* spheres forming a cubic lattice, hexagonally packed rods, or, in case of compositionally symmetric diblock copolymers ($f = 0.5$), a lamellar structure [1]. Below $(\chi N)_{\mathrm{ODT}}$, the chains form a disordered melt with some correlation on a length scale of the order of the radius of gyration. For symmetric diblock copolymers, the ODT is predicted by mean-field theory to be a critical point at $\chi N = 10.5$ [2]. When fluctuations are included in the calculations, $(\chi N)_{\mathrm{ODT}}$ becomes weakly N-dependent and the ODT becomes weakly first order [2, 3]. In addition, recent experimental work has established the importance of configurational asymmetry [4].

The scaling relation between the characteristic length and the chain length in diblock copolymer systems has gained considerable interest. In the mean-field theory of Leibler [2], the chains are assumed to be Gaussian and thus the scaling exponent δ is $1/2$ in the ordered state close to the ODT, where the concentration profile is sinusoidal [2]. This regime is often refered to as the Weak-Segregation Limit (WSL). We find the definition of this term ambiguous, which will be discussed below. In the Strong-Segregation Limit (SSL) deep in the ordered state, exponents of 0.643 [5] and $2/3$ [6, 7] have been predicted for symmetric diblock copolymers (lamellar morphology). The first value has been obtained by Helfand and Wasserman in a partially numerical, self-consistent field calculation, assuming narrow interphases [5]. The contributions included in the free energy are the enthalpic interactions in the interphase and the entropy losses due to chain stretching and joint localization. $\delta = 0.643$ has been obtained for a completely symmetric lamellar system. The entropy loss related to joint localization is generally neglected, because it only varies weakly with D compared to the two other terms. $\delta = 2/3$ has been obtained by Semenov in an analytical approach based on analogy with electrostatics [6] and by Ohta and Kawasaki, who calculate the entropy loss due to chain stretching in a mean-field approach, using a random-phase approximation [7].

We have recently investigated the crossover from Gaussian scaling to the SSL [8]. We have found that there exists an intermediate regime with an exponent higher than in the two bordering regimes, *i.e.* the characteristic length varies more strongly with χN in the intermediate regime than in the SSL. In the present publication, we discuss in greater detail the methods applied to obtain thermal equilibrium as well as the change of the lamellar correlation length and the concentration profile with varying chain length. In addition, a study of the temperature behavior around the ODT is presented.

Several recent theoretical mean-field approaches address the scaling behavior in the ordered state [9–15]. In these studies, the variation of the lamellar thickness with chain length is found to be stronger in the vicinity of the ODT than both in the Gaussian regime and in the SSL, δ being here between 0.72 [9, 12] and 1.071 [14]. For large values of χN, the variation of the lamellar thickness is found to approach SSL behavior ($D \propto N^{2/3}$) asymptotically. Extrapolating from the regime near the ODT and from the SSL, χN-values between 17 [14] and 95 [9] are identified for the crossover between the intermediate regime and the SSL. The change in scaling behavior in the ordered state is predicted to be closely linked to chain stretching [15] and to the coarsening of the concentration profile, which evolves from being sinusoidal close to the ODT to being rectangular as χN increases [9–11, 15]. In two cases, a true scaling regime linking the WSL (close to the ODT) and the SSL is predicted [9, 12]. These theories recover the WSL result of $\delta = 1/2$ in the ordered state close to the ODT [9, 12]. This is in contradiction to experiments [8, 16–18], where the intermediate-segregation regime has been found to reach into the disordered state (down to $\chi N \simeq 5 - 6$) with Gaussian scaling encountered below this value. Deviations from Gaussian scaling already in the disordered state have been predicted by fluctuation theories [19, 20]. Thus, the term "WSL" is ill-defined: in the ordered state near the ODT, the concentration profile of one block is sinusoidal, but the scaling exponent is higher than $1/2$, *i.e.* both WSL criteria are not fulfilled. We will therefore not use this term in

the present publication and will instead refer to this regime as the Intermediate-Segregation Regime (ISR) and to the regime for $\chi N < (\chi N)_{GST}$, the Gaussian-to-stretched-coil transition, as the Gaussian regime. It should be noted that the location of $(\chi N)_{GST}$ is predicted to depend on the Ginzburg parameter (*e.g.* [4]) $\bar{N} = N\bar{a}^6/v^2$ ($\bar{a}$ and v denote the average segment length and the reference segment volume), which is proportional to the chain length, N: the larger N, the closer the GST is to the ODT [19,20].

Before the advent of the theories cited above, several experimental studies addressed the scaling behavior of the characteristic length in the lamellar state, resulting in very different values of the exponent [16, 18, 21–23]. Hashimoto *et al.* [21] and Richards and Thomason [22] studied lamellar polystyrene-polyisoprene samples, which were prepared by solvent-casting from toluene at room temperature, *i.e.* below the glass temperature of the polystyrene block (*ca.* 100 °C). Hashimoto *et al.* found their results (obtained using samples having molar masses between 21 000 and 102 000 g/mol) consistent with an exponent of 2/3, whereas Richards and Thomason found $\delta = 0.56$ [22] by fitting a power law to the data (molar masses between 16 720 and 178 100 g/mol, including triblock copolymers). It should be noted that during solvent-casting, a certain degree of order may be achieved while solvent is still present and this non-equilibrium state may freeze in when the solvent evaporates. This may be particularly severe when solvent-casting below the upper glass temperature of the block copolymers. Hadziioannou and Skoulios [18] also investigated symmetric polystyrene-polyisoprene samples, but prepared macroscopically oriented samples using shear alignment with subsequent annealing above the glass temperature of both blocks. The molar mass range covered was 27 000-205 000 g/mol, leading to $\delta = 0.79 \pm 0.02$. Almdal *et al.* studied a series of poly(ethylene-propylene)-poly(ethylethylene) ($N = 125 - 1890$), the samples being annealed above their upper glass temperature and found $\delta = 0.80 \pm 0.04$ [16]. Matsushita *et al.* studied polystyrene-poly(vinylpyridine) having molar masses between 38 000 and 739 000 g/mol, which were solvent-cast at room temperature and found $\delta = 0.64$ [23]. The discrepancies may have different origins: chemically different samples were studied, different ranges in phase space were explored and different sample preparation methods were used, of which some might have led to non-equilibrium structures.

The present study is motivated by the fact that the experimentally determined exponents differ substantially and that, in spite of the large number of studies, the crossover from the intermediate-segregation regime near the ODT to the SSL has not been experimentally confirmed. A homologous series of compositionally symmetric polystyrene-polybutadiene diblock copolymers spanning a wide range in chain lengths is investigated, with the aim of identifying and localizing the crossover from the ISR to the SSL. The conditions under which thermal equilibrium can be obtained are established by preparing the ordered samples using the methods applied in the experimental studies cited above: annealing, solvent-casting as well as shear alignment, all above the highest glass temperature. The dependence of the sample structure on the chain length and the preparation method applied is investigated using small-angle X-ray (SAXS) and neutron scattering (SANS). The scaling behavior of the characteristic length with chain length is determined and the crossover from an intermediate-segregation regime to the SSL is identified. This change of scaling behavior is found to be related to the change of the shape of the concentration profile. A narrow range of the phase space around the ODT is studied by monitoring the temperature dependence of the SANS spectra of a low molar-mass sample. We finish by presenting a three-regime picture of the scaling of the characteristic length with χN.

2. Experimental

2.1. SYNTHESIS. — A homologous series of ten symmetric polystyrene-polybutadiene (SB) diblock copolymers having molar masses between 9 200 and 183 000 g/mol was synthesized using anionic polymerization under an atmosphere of purified argon [24]. Styrene, 1,3-butadiene, and cyclohexane (all from Aldrich, 99%) were purified as described in reference [24]. *Sec*-butyl lithium (Aldrich) was chosen as the initiator for the polymerization, which was carried out at 40 °C and was terminated using degassed methanol. The polymer was precipitated in a 2:1 mixture of methanol and 2-propanol, a poor solvent for SB. The solvent was poured off and the polymer sample was dried at room temperature under vacuum. The yield was larger than 93% for nearly all samples (Tab. I). Thus, the resulting molar masses agree with those based on stoichiometry within a few percent. The degree of polymerization, N, was calculated based on the volume of the polybutadiene monomer, $v = M_B/\rho_{PB}$.

$$N = \frac{M_{PB}/\rho_{PB} + M_{PS}/\rho_{PS}}{M_B/\rho_{PB}} \tag{1}$$

where M_{PB} and M_{PS} are the molar masses of the polybutadiene and the polystyrene block, calculated from stoichiometry, and M_B the molar mass of the butadiene monomer. $\rho_{PS} = 1.05$ g/cm^3 [25] and $\rho_{PB} = 0.89$ g/cm^3 [26] are the mass densities of polystyrene and polybutadiene. A range $N = 156 - 3\,090$ is covered with the samples investigated (Tab. I).

2.2. CHARACTERIZATION. — The polymer microstructure was determined with ^{1}H NMR spectroscopy using a Bruker AC-250 MHz instrument [27]. The samples were dissolved in d-chloroform (30 mg/ml). An amount of 91% 1,4-addition of polybutadiene was found, the remainder resulting from 1,2-addition. The weight fraction of polystyrene is $w_{PS} = 0.55 \pm 0.01$ for all samples, corresponding to volume fractions $f_{PS} = 0.51 \pm 0.01$, using the densities given above. The block copolymers are thus close to symmetric.

The glass temperatures of the samples were determined in differential scanning calorimetry experiments. For this purpose, a Perkin-Elmer DSC-4 instrument operated at a heating rate of 40 °C/min was used. Prior to the measurements, the samples were heated to 150 °C.

For dynamic mechanical measurements, an RMS-800 rheometer (Rheometrics) operated in the parallel-plate geometry was used. Pills of *ca.* 1 mm thickness were pressed and mounted between the plates. The samples were thermally equilibrated in a stream of nitrogen gas. The ODT temperatures of the low molar mass samples were determined from the drop of the dynamic elastic and loss modulus in heating runs (Fig. 1), applying heating rates between 0.1 and 3.0 °C/min, shear frequencies between 0.02 and 40.0 rad/s and shear amplitudes of 2 or 5% [28]. The values of T_{ODT} are given in Table I.

The molar-mass distributions were measured using size exclusion chromatography. A Knauer system together with a PL-precolumn, a 100 cm Shodex A-80M column and a high temperature differential refractometer was used. The molar-mass distributions of untreated samples were narrow: $\bar{M}_w/\bar{M}_n \leq 1.1$, where $\bar{M}_w$ denotes the weight-average and $\bar{M}_n$ the number-average molar mass.

2.3. SAMPLE PREPARATION. — The temperature chosen for the preparations and for most measurements was 150 °C. In order to prevent the samples from crosslinking during the preparations and measurements, where the samples were at high temperature for a long time, they were stabilized by adding 0.1 or 0.5 wt-% (relative to the polymer mass) of antioxidant (Irganox 1010, Ciba-Geigy), see Table I. The polymer samples were dissolved together with Irganox 1010

Table I. — *Sample characteristics.* M_n^{stoich} *· stoichiometric molar mass. N: degree of polymerization based on the polybutadiene segment volume. The content of antioxidant is given in weight-% per polymer mass.* $\bar{M}_w/\bar{M}_n$*: after sample preparation, from size exclusion chromatography. CHx stands for cyclohexane. (a) Outside the accessible temperature range, (b) not determined.*

sample	M_n^{stoich} (g/mol)	N	yield (%)	T_{ODT} (°C)	Irganox content (wt-%)	preparation method	$\bar{M}_w/\bar{M}_n$
SB05	9200	156	94	(a)	0.1	disordered	1.10
SB14	13900	236	65	71 ± 1	0.1	disordered	1.08
SB11	18300	310	93	130 ± 2	0.1	disordered	1.08
SB01	18500	313	95	146 ± 2			1.09
SB12	22100	374	(b)	181 ± 2	0.1	annealed	1.14
					0.1	solvent-cast from benzene	1.12
					0.1	shear aligned (1.0 rad/s)	(b)
SB08	22600	383	(b)	204 ± 2	0.1	annealed	1.09
					0.1	solvent-cast	1.16
					0.1	shear aligned (1.0 rad/s)	(b)
SB02	54500	921	98	(a)	0.1	annealed	1.20
					0.1	solvent-cast from benzene	1.27
					0.1	shear aligned (1.0 rad/s)	1.10
SB15	69900	1182	(b)	(a)	0.1	annealed	1.16
					0.1	solvent-cast from benzene	1.15
					0.1	shear aligned (1.0 rad/s)	1.07
SB06	91900	1555	95	(a)	0.1	solvent-cast from benzene	1.22
					0.1	shear aligned (1.0 rad/s)	1.09
					0.5	annealed	1.12
					0.5	solvent-cast from benzene	1.13
					0.5	solvent-cast from CHx	1.12
SB07	148000	2511	98	(a)	0.5	annealed	1.26
					0.5	solvent-cast from benzene	1.18
					0.5	solvent-cast from CHx	1.23
					0.5	shear aligned (0.02 rad/s)	1.16
SB10	183000	3090	99	(a)	0.5	annealed	1.31
					0.5	solvent-cast from benzene	1.27
					0.5	shear aligned (0.02 rad/s)	1.16

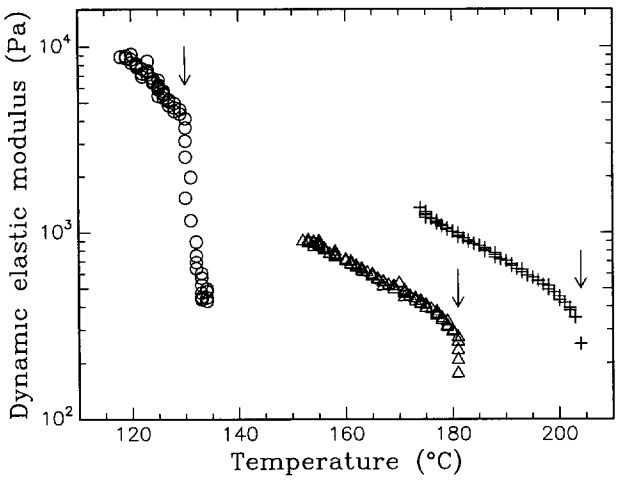

Fig. 1. — The dynamic elastic modulus as a function of temperature in a semilogarithmic representation. The arrows indicate the ODT temperatures assigned. Circles: $N = 310$, heating rate 1.0 °C/min, shear frequency 10 rad/s, shear amplitude 5%. Triangles: $N = 374$, 1.0 °C/min, 10 rad/s, 2%. Plusses: $N = 383$, 3.0 °C/min, 40 rad/s, 5%.

in benzene and stirred for some hours. The solutions were left to dry at room temperature. Remaining solvent was removed by keeping the samples at 100 °C under vacuum for 2 hours.

Samples being disordered at 150 °C were pressed in a teflon-coated press (1 mm thick pills) and were left to equilibrate for 15 min at 150 °C prior to the measurements. Ordered samples were prepared using different methods: annealing, solvent-casting and shear alignment (Tab. I). Annealing of pressed pills at 150 °C for two days under vacuum results in "polycrystalline" samples, *e.g.* the lamellar domains are randomly oriented. Solvent-casting is a method used to prepare macroscopically oriented samples (*e.g.* [21]). The orientation is induced by the film surfaces with the lamellar interfaces aligning parallel to these. The samples were dissolved in benzene, a good, non-selective solvent (40-90 mg/ml). The solutions were left to dry in teflon beakers at room temperature for some days, resulting in films of *ca.* 0.6 mm height. The films were annealed for two days at 150 °C under vacuum. Additionally, two samples were solvent-cast from cyclohexane which, at room temperature, is a marginal solvent for polystyrene and a good solvent for polybutadiene. Shear alignment is another technique for macroscopically orienting samples [29]. Pills were pressed and mounted in a shear sandwich fixture (pill size 12.5 × 16 × 0.5 mm^3) of an RSA II rheometer (Rheometrics Solids Analyzer). They were subject to oscillatory shear with amplitudes of 20-100% for 1-4 hours at 150 °C. High molar mass samples were sheared at frequencies of 0.02 rad/s and low molar mass samples at 1.0 rad/s, see Table I. All shear aligned samples were oriented with the lamellar interfaces perpendicular to the shear gradient direction.

A minor degree of crosslinking occured during preparation (typically 5-7% dimers and trimers), as indicated by size exclusion chromatography. However, the molar-mass distributions are still narrow: $\bar{M}_w/\bar{M}_n$ is typically below 1.2 after preparation (Tab. I).

2.4. SANS. — SANS experiments were carried out at the Risø SANS facility. The following neutron wavelengths λ and sample-detector distances were used: 14.8 Å/6 m,

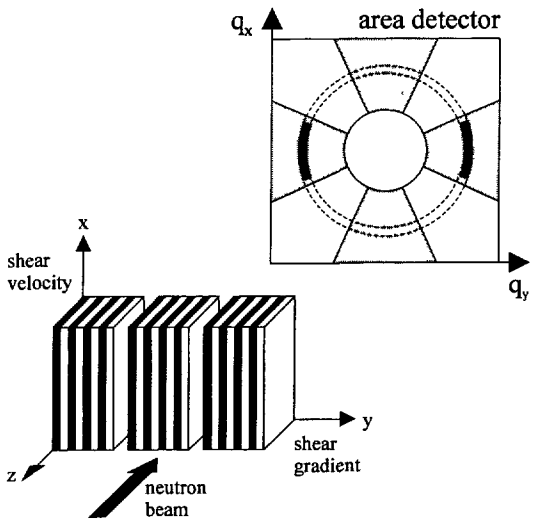

Fig. 2. — The experimental geometry in SANS experiments with shear aligned samples. The shear velocity and the shear gradient directions are parallel to the x- and the y-direction, respectively. Note that the lamellar thickness is much smaller than the thickness of the sample slices and that the lamellar structure may display defects. Solvent-cast samples were mounted in the same way. The neutron beam hits the sample in z-direction. The black arcs on the detector indicate the first-order diffraction peaks and the dashed circles the underlying Debye-Scherrer ring. The sector masks in q_x- and q_y-direction (shaded areas) are used for averaging the SANS spectra. The circle in the middle indicates the beamstop which is masked away.

7.67 Å/6 m and 5.58 Å/3 m. $\Delta\lambda/\lambda$ was 9% in all cases. The q-ranges covered were $q \simeq 0.0032 - 0.018$ Å^{-1}, $0.0054 - 0.035$ Å^{-1} and 0.013-0.10 Å^{-1}, respectively. Samples were mounted between aluminum foil in a furnace which was surrounded by air. The temperature was computer-controlled with a stability better than 0.5°C. Disordered and annealed samples were mounted with the neutron beam perpendicular to the pill surface. Solvent-cast and shear aligned samples were cut in stripes, stacked and mounted in the neutron beam as shown in Figure 2. In both cases, the sample thickness was $\sim$ 0.5-1 mm. The measuring times were between a few minutes and one hour. The two-dimensional spectra of disordered samples display broad rings, corresponding to a broad correlation peak. Typical two-dimensional SANS spectra of an ordered sample prepared in different ways are shown in Figure 3. With ordered annealed samples, first-order Debye-Scherrer rings are observed. Spectra from solvent-cast and shear aligned samples show first-order Bragg-reflections on each side of the direct beam on top of a diffraction ring, attributed to remaining unoriented material. Data analysis was made using standard Risø software [30]. The spectra were azimuthally averaged and the background from aluminum foil and the dark current were subtracted. When averaging spectra from solvent-cast and shear aligned samples, sector masks were used having opening angles of 30° in the q_y-direction (through the peaks) or in the q_x-direction (Fig. 2).

2.5. SAXS. — SAXS experiments were carried out at Roskilde University using a Kratky compact-camera mounted on a sealed X-ray tube with a one-dimensional position-sensitive detector. A description of the instrument is given in [27, 28]. The accessible q-range is $\sim 0.007 - 0.55$ Å^{-1} Samples were mounted between kapton foil in a teflon-coated, tem-

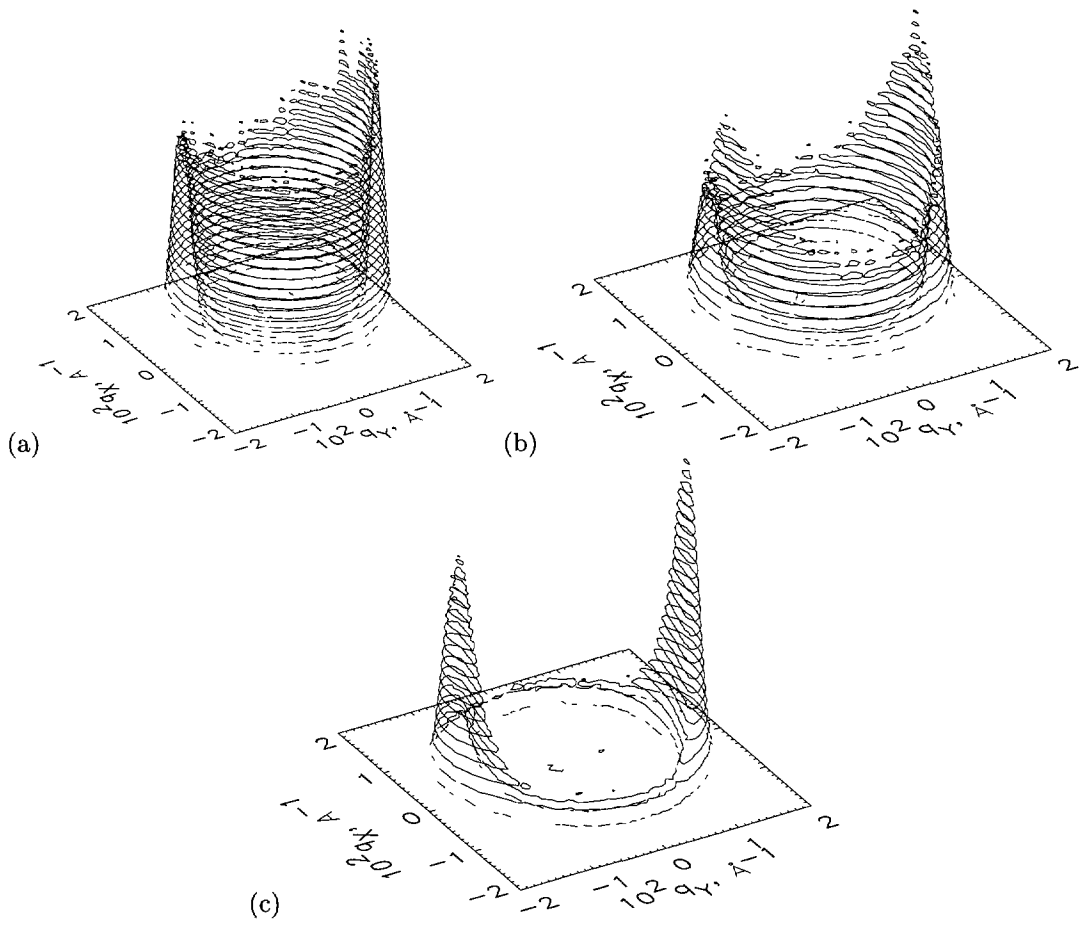

Fig. 3. — Two-dimensional SANS spectra from a sample having $N = 1182$, being prepared in different ways. The spectra were measured at 150 °C and were not normalized. The lines are linearly spaced isointensity lines. (a) Annealed, (b) solvent-cast, (c) shear aligned (the sample was slightly misaligned when mounted in the neutron beam).

perature controlled sample holder with a temperature stability better than 0.2 °C. Disordered and annealed samples were mounted with the X-ray beam perpendicular to the pill surface. Solvent-cast and shear aligned samples were mounted as shown in Figure 4. Shear-aligned samples were additionally rotated by 90° around the x-axis, *i.e.* with the beam perpendicular to the lamellar interfaces. The sample thickness was *ca.* 1 mm. Measuring times were between 500 and 2000 s. The background scattering from kapton film was subtracted.

Additional SAXS measurements on two disordered samples were made using a pinhole camera mounted on a rotating anode at the Service de Chimie Moléculaire, Centre d'Energie Atomique, Saclay, which has a Huxley-Holmes collimation section and a two-dimensional multiwire detector [31]. The q-range is $\sim 0.01 - 0.7$ Å^{-1} Samples were mounted between kapton in the sample holder used for measurements with the Kratky-camera. The background scattering arising from kapton film was subtracted from the spectra. The spectra were azimuthally averaged and Lorentz-functions were fitted to the resulting peaks.

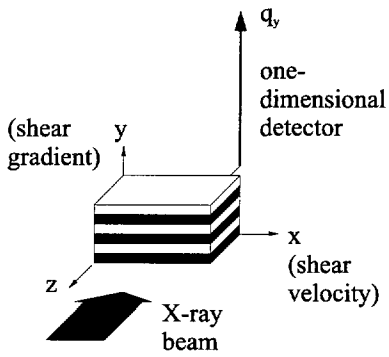

Fig. 4. — Illustration of the experimental geometry in SAXS experiments (using the Kratky-camera) with shear aligned samples. The beam hits the sample in z-direction and has its length dimension in x-direction. Scattering is measured in the q_y-direction. Solvent-cast samples were mounted in the same way. Shear aligned samples were also mounted rotated 90° around the x-axis.

3. Results and Discussion

3.1. The Choice of Measuring Temperature. — Knowledge of the glass transition temperatures of the diblock copolymer samples is necessary in order to avoid measurements in the glassy state, where mechanical tensions and thus non-equilibrium states may persist. The glass transition temperatures depend on the block copolymer molar mass and on the degree of segregation (*e.g.* [32]). The glass transition temperature of pure polystyrene is $\sim$ 100 °C or lower, depending on the molar mass [25], and the glass transition temperature of pure polybutadiene is between −107 and −83 °C, depending on the microstructure [25]. In strongly segregated diblock copolymer systems, two glass transitions are expected, one for each block. In the fully homogeneous, disordered state, only one glass transition is expected, located between the transition temperatures of the pure blocks.

In differential scanning calorimetry experiments, the upper glass transition temperatures of two SB samples were determined. Values of 76 °C and 102 °C were found for $N = 374$ and $N = 921$, respectively. At these temperatures, the samples are in the ordered state. The glass transition temperatures of samples having $N > 921$ are expected to be close to the values for the pure blocks, because these samples are strongly segregated. The upper glass transition temperatures of samples having $N < 374$ could not be determined unambiguously, probably because of the interplay between the partial segregation and the glass transition.

The temperature for preparations and measurements (except for the temperature scan, see Sect. 3.8) was chosen to be 150 °C, *i.e.* well above the glass transition temperatures of the two blocks.

3.2. Determination of the Segment-Segment Interaction Parameter. — The ODT temperatures of five low molar mass samples were determined in dynamic mechanical measurements (Tab. I). The feature defining the ODT temperature (T_{ODT}) is the drastic drop in the dynamic elastic and loss modulus (Fig. 1). Using the mean-field prediction for symmetric diblock copolymers, $(\chi N)_{\mathrm{ODT}} = 10.5$ [2], together with the relationship $\chi = A/T + B$ [33], where T is the temperature, it is found that

$$T_{\mathrm{ODT}} = \frac{AN}{10.5 - BN}. \tag{2}$$

Note that the values of A and B depend on the definition of N (Eq. 1). A least-square fit of the expression from equation 2 to the experimentally determined ODT temperatures gives $A = (21.6 \pm 2.1)$ K and $B = -0.019 \pm 0.005$.

Using instead the expression given by fluctuation theory [3]

$$(\chi N)_{\mathrm{ODT}} = 10.5 + 41.0 \left(\frac{N \bar{a}^6}{v^2} \right)^{-1/3} \tag{3}$$

with the polybutadiene monomer volume $v = 101$ Å^3 and the average segment length $\bar{a} = 6.1$ Å, we find $A = (31.3 \pm 3.0)$ K and $B = -0.031 \pm 0.007$. $\bar{a}$ was found by weighting the segment lengths of polystyrene and polybutadiene, a_{PS} and a_{PB}, by their respective volume fractions:

$$\bar{a}^2 = f_{\mathrm{PS}} a_{\mathrm{PS}}^2 + (1 - f_{\mathrm{PS}}) a_{\mathrm{PB}}^2 \tag{4}$$

with $f_{\mathrm{PS}} = 0.5$ and

$$a_{\mathrm{PB}}^2 = \langle R^2 \rangle_0^{\mathrm{PB}} \frac{M_{\mathrm{B}}}{\mathrm{M_{PB}}}, \tag{5}$$

$$a_{\mathrm{PS}}^2 = \langle R^2 \rangle_0^{\mathrm{PS}} \frac{M_{\mathrm{B}}/\rho_{\mathrm{PB}}}{\mathrm{M_{PS}}/\rho_{\mathrm{PS}}} \cdot \tag{6}$$

Here, we inserted the values of the unperturbed mean-square end-to-end distances of the two blocks, $\langle R^2 \rangle_0^{\mathrm{PB}}/M_{\mathrm{PB}} = 0.876$ Å^{2}mol/g and $\langle R^2 \rangle_0^{\mathrm{PS}}/M_{\mathrm{PS}} = 0.434$ Å^{2}mol/g [26]. The second term in equation 6 represents the inverse of the number of polystyrene units having the same volume as the reference monomer. At 150 °C, we thus get $\chi = 0.033 \pm 0.007$ and 0.043 ± 0.010 using the mean-field and the fluctuation expression, respectively. In the following, the mean-field result is used, leading to $N_{\mathrm{ODT}} = 323$, *i.e.* only samples with $N > 323$ are expected to be ordered.

3.3. The Degree of Orientation. — After the synthesis, the polymer samples are precipitated in a poor solvent. For samples being ordered at room temperature, this corresponds to a rapid quench from the dissolved into the ordered state and these samples are thus not necessarily in an equilibrium state. Further treatment is therefore necessary in order to ensure thermal equilibrium. As the ODT temperatures of the high molar mass samples are above the degradation temperature (*ca.* 200 °C), it is not possible to heat these samples above the ODT temperature and to cool them down to the ordered state again, but other methods are necessary in order to achieve thermal equilibrium. All ordered samples were therefore annealed, solvent-cast and shear aligned following the procedures described in the Experimental Section.

SANS spectra from annealed samples are isotropic (Fig. 3a) and were azimuthally averaged. SANS spectra from solvent-cast and shear aligned samples were analyzed using sector masks, monitoring the intensity in the q_x- and q_y-direction (Figs. 2, 3b and 3c). Lorentz-functions

$$I(q) = I_{\mathrm{bg}} + \frac{I_o}{1 + (q - q^*)^2 \xi^2} \tag{7}$$

were smeared with the instrumental resolution and fitted to the peaks [30] (I_{bg} denotes a constant background, I_{o} the peak height, q^* the peak position, and ξ the inverse half width at half maximum). The differences in the peak positions in the q_y- and the q_x-directions are typically smaller than 2%. In Figure 5, azimuthally averaged spectra from shear aligned samples having different chain lengths are shown together with the smeared and fitted Lorentz-functions. For nearly all solvent-cast and for all shear aligned samples, the peak height in

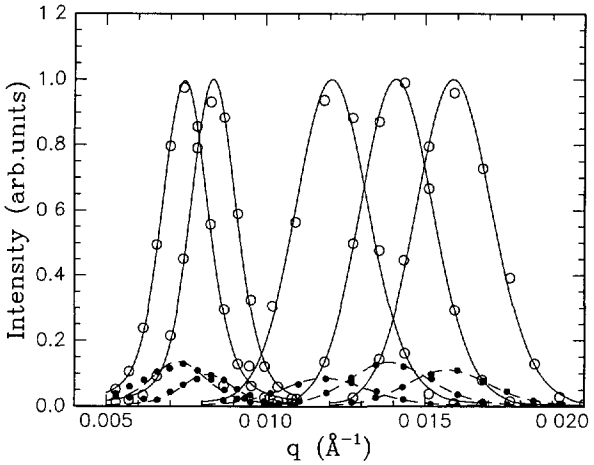

Fig. 5. — Azimuthally averaged SANS spectra of shear aligned samples measured at 150 °C. The background is subtracted. From left to right: $N = 3090$, 2511, 1555, 1182, and 921. (○) q_y-direction, (•) q_x-direction. The error bars are smaller than the symbol size. The spectra were measured with two different settings (14.8 Å/6 m for $N = 3090$ and 2511 and 7.67 Å/6 m for the other samples). The data are normalized to a peak height of unity. The lines are fits of Lorentz-functions convoluted with the instrumental resolution to the q_y-spectra (full lines) and the q_x-spectra (broken lines).

the q_y-direction, I_0^y, is higher than the one in the q_x-direction, I_0^x, *i.e.* solvent-cast samples are oriented with the lamellar interfaces parallel to the film surface and shear aligned samples with the lamellar interfaces perpendicular to the shear gradient (Figs. 2, 3b and 3c). In case of solvent-cast samples, the intensity ratios I_0^y/I_0^x are found to be $\sim 2 - 4$. indicating a relatively low degree of alignment (Fig. 3b). The reason might be that the film thicknesses (approximately 0.6 mm) were large compared to the lamellar thickness (a factor of $7\,000 - 30\,000$). This indicates that the lamellae are well-oriented close to the film surfaces and that the orientation is gradually lost towards the bulk. With shear aligned samples, the ratios are higher, $I_0^y/I_0^x \simeq 11 - 28$, the alignment is thus better than for solvent-cast samples (Fig. 3c). We conclude that under the conditions present under shear alignment (Tab. I), relatively good macroscopic orientation is achieved. However, high molar mass samples are mechanically hard and therefore difficult to align macroscopically.

3.4. The Lamellar Correlation Length. — The lamellar correlation length is estimated from the width of the first-order Bragg-reflections observed in the SANS spectra, as explained below. It should be noted that block copolymer systems display sharp domain boundaries as well as a gradual loss of lamellar orientation (*e.g.* [34]). A model of the scattering from a lamellar structure is given in the appendix, leading to a relationship between the number of correlated lamellae, N_s, and the width of the first-order Bragg peak. As we in the following analysis only need the peak positions and the peak widths, we fitted Lorentz-functions (Eq. 7) to the peaks measured in small-angle scattering experiments instead of the expressions given in equations (A.3 and A.4) together with equations (A.6 and A.8). In some cases, a slanted background was added in order to account for residual background scattering in SAXS spectra. N_s is then given by

$$N_s \simeq \frac{2.75\, q^* \xi}{2\pi} \tag{8}$$

where we identify $q_H = 1/\xi$.

N_s as a function of chain length, N, is shown in Figure 6 for annealed, solvent-cast and shear aligned samples. In the case of annealed samples, the azimuthally averaged and background-corrected scattered intensity should in principle be multiplied with the Lorentz-factor for polycrystalline samples $4\pi q^2$ [35]. As the peaks obtained in the present study were relatively narrow, this correction only leads to minor changes in the peak shape and position and is thus omitted.

We find that in annealed samples, $8-24$ lamellae are on average correlated orientationally. Approximately the same values are obtained with solvent-cast ($N_s = 5-17$) and shear aligned samples in the q_x-direction ($N_s = 5-18$), *i.e.* from the unoriented material. The number of correlated lamellae in the q_y-direction is higher: $N_s = 7-63$ for solvent-cast and $N_s = 10-59$ for shear aligned samples, in accordance with the observations made using electron microscopy (*e.g.* [34]).

For samples prepared in either way, N_s is largest for moderate molar masses (Fig. 6). In the vicinity of the ODT (only measured with annealed and solvent-cast samples). N_s is relatively low. We do not believe this phenomenon to be related to the change in concentration profile close to the ODT, since the peak width only weakly depends on the shape of the concentration profile. A possible explanation is that samples which are close to the ODT contain many defects, the resulting domains being smaller than deeper in the ordered state. Also, a distribution of the lamellar thickness may increase the peak width. The broader the distribution of lamellar thicknesses, the smaller ξ, *i.e.* the number of correlated lamellae is underestimated when this distribution is not taken into account. Samples with high chain lengths ($N = 2\,511-3\,090$) also display relatively small values of N_s. As the mobilities of long chains are low, the formation of domains is a slow process. Both entanglement effects and the strong repulsive interactions between different blocks may play a role. Longer annealing possibly leads to an increase of the number of correlated lamellae. However, in the present study, the annealing times were chosen to be no longer than two days in order to avoid crosslinking of the polybutadiene blocks.

3.5. The Concentration Profile in the Ordered State. — In the SAXS experiments, the q-range studied was larger than in SANS. Thus, higher-order reflections could be detected, making the characterization of the concentration profile possible. For desmearing, the routine ITR [36] was used. Spectra from annealed samples were desmeared with respect to the beam length effect (Fig. 7), but were resolution-limited with respect to the beam width. SAXS spectra from shear aligned samples are shown in Figure 8 in the q_y- and the q_z-direction. In general, the spectra measured in the q_y-direction display sharp and nearly symmetric peaks, whereas more flat and asymmetric peaks are obtained in q_z-direction. In the q_y-direction, the scattering from oriented lamellar domains is monitored. Spectra from oriented, "single-crystalline" samples are not affected significantly by beam length smearing and were therefore not desmeared. Lorentz-functions on top of a slanted background were fitted to the peaks, the background accounting for residual beam length smearing (Fig. 9). In the q_z-direction, scattering from unoriented parts of the sample is measured and these spectra are affected by beam length smearing, which for sharp peaks leads to asymmetric smeared peak shapes [36] (Fig. 7). Especially for the samples with larger chain lengths ($N = 921-1555$), this effect is clearly observed. Spectra from solvent-cast samples were treated in the same way as the ones from shear aligned samples. The peak positions of ordered samples were determined as follows: when only one peak is present, the position of this peak is used: $q^* = q_1$. When higher-order Bragg-reflections appear, the third-order reflections are used ($q^* = q_3/3$), because of the lower relative error of q_3 (Tab. II).

The higher the chain length, the more pronounced are the higher-order reflections (Fig. 8), *i.e.* the closer to rectangular are the concentration profiles. For the samples having $N = 374$

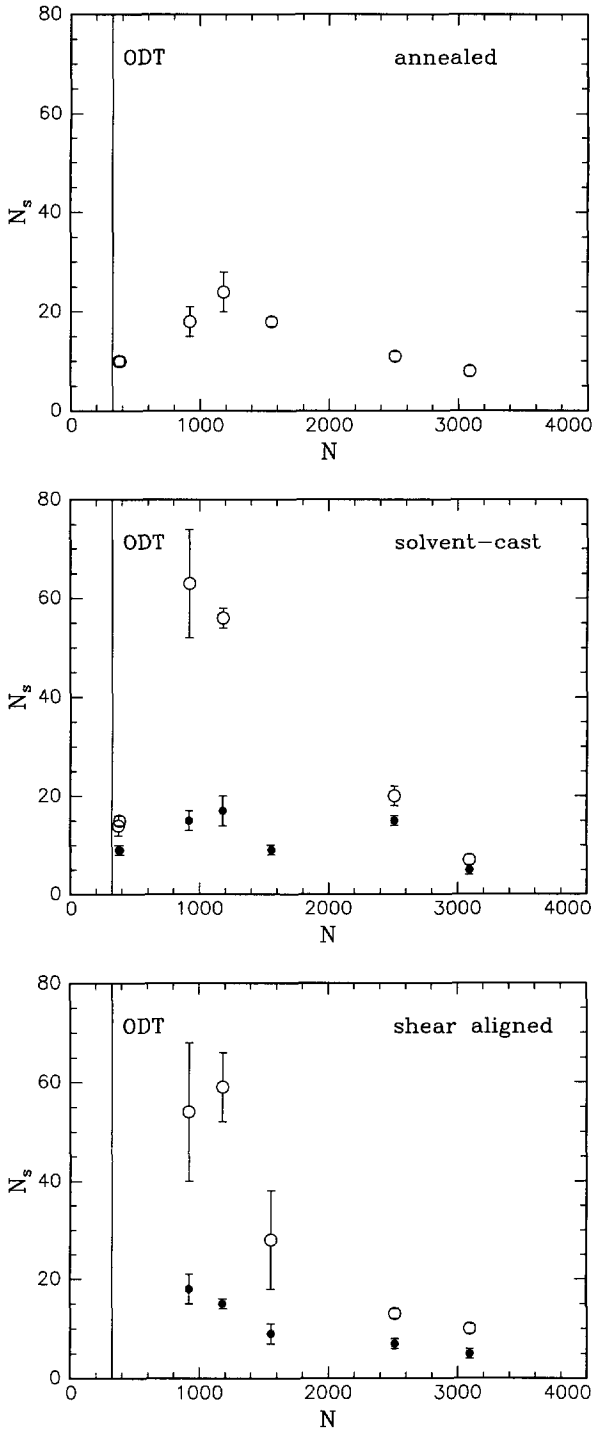

Fig. 6. — Number of correlated lamellae, N_s, as a function of chain length, N, for different sample preparation methods. The vertical line indicates N_{ODT}. For solvent-cast and shear aligned samples: (○) q_y-direction, (●) q_x-direction.

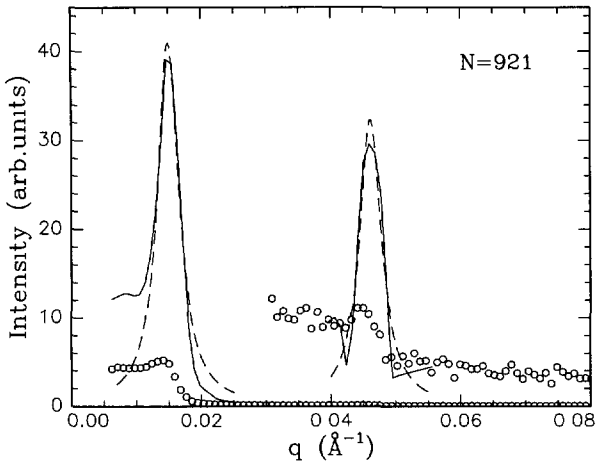

Fig. 7. — Background-corrected SAXS spectrum from an annealed sample measured at 150 °C using the Kratky-camera. (o) Experimental data, full line: desmeared spectrum, dashed line: fits of Lorentz-functions to the first- and third-order Bragg-peaks. For $q > 0.03$ Å^{-1}, the intensities are multiplied with a factor of 100 in order to reveal the third-order Bragg-peak.

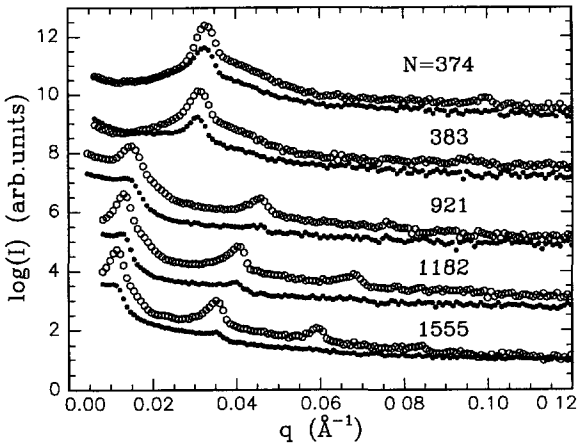

Fig. 8. — Semi-logarithmic plot of background-corrected SAXS spectra from shear aligned samples, measured at 150 °C using the Kratky-camera. (o) q_y-direction, (•) q_z-direction. The spectra are shifted by arbitrary amounts.

and $N = 383$, only the first-order Bragg-reflection can be distinguished from the background, indicating that the concentration profile is close to sinusoidal. The gradual change from a sinusoidal profile close to the ODT to a rectangular profile corresponds to a gradual decrease of the interfacial width and is consistent with theoretical predictions [9–11, 15].

3.6. Solvent Selectivity. — In order to establish whether the final structure depends on the selectivity of the solvent used in the solvent-casting procedure, SAXS and SANS measurements were additionally made on two samples solvent-cast from cyclohexane, which is a

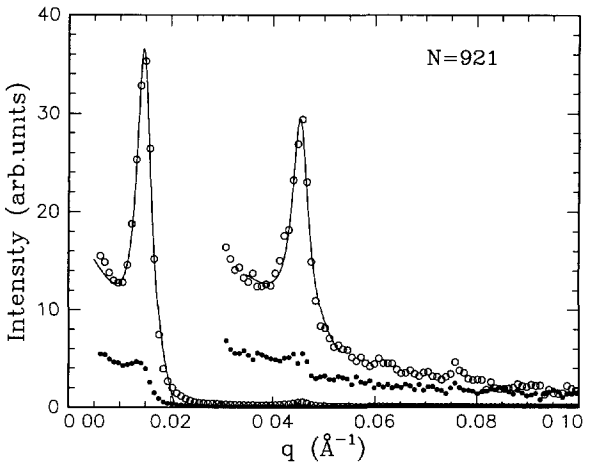

Fig. 9. — Background-corrected SAXS spectra from a shear aligned sample measured at 150 °C using the Kratky-camera. (○) q_y-direction, (●) q_z-direction. The lines are fits of Lorentz-functions on a slanted background to the first and third-order Bragg-peaks in the q_y-spectrum. The intensities for $q > 0.03$ Å^{-1} are multiplied with a factor of 50 in order to reveal the third-order Bragg-reflection.

Table II. — *Peak positions at 150 °C in 10^{-2}Å^{-1} as determined in small-angle scattering experiments. ([a]) Solvent-cast from benzene. ([b]) Kratky-camera, ([c]) SANS, ([d]) SAXS pinhole camera. For solvent-cast and shear aligned samples, the q_y-values are given.*

sample	N	disordered	annealed	solvent-cast[a]	shear aligned
SB05	156	6.20 ± 0.09^b			
		6.10 ± 0.17^d			
SB14	236	4.55 ± 0.09^b			
SB11	310	3.98 ± 0.09^b			
		3.85 ± 0.11^c			
		3.93 ± 0.17^d			
SB12	374		3.33 ± 0.04^b	3.33 ± 0.04^b	3.32 ± 0.02^b
			3.32 ± 0.11^c	3.35 ± 0.11^c	$-^c$
SB08	383		3.18 ± 0.04^b	3.13 ± 0.04^b	3.12 ± 0.02^b
			3.19 ± 0.11^c	3.20 ± 0.11^c	$-^c$
SB02	921		1.54 ± 0.02^b	1.48 ± 0.02^b	1.51 ± 0.02^b
			1.57 ± 0.04^c	1.58 ± 0.04^c	1.59 ± 0.04^c
SB15	1182		1.37 ± 0.02^b	1.33 ± 0.02^b	1.34 ± 0.02^b
			1.41 ± 0.04^c	1.40 ± 0.04^c	1.41 ± 0.04^c
SB06	1555		1.19 ± 0.02^b	1.19 ± 0.02^b	1.17 ± 0.02^b
			1.20 ± 0.04^c	1.23 ± 0.04^c	1.21 ± 0.04^c
SB07	2511		0.839 ± 0.022^c	0.832 ± 0.022^c	0.837 ± 0.022^c
SB10	3090		0.753 ± 0.022^c	0.747 ± 0.022^c	0.748 ± 0.022^c

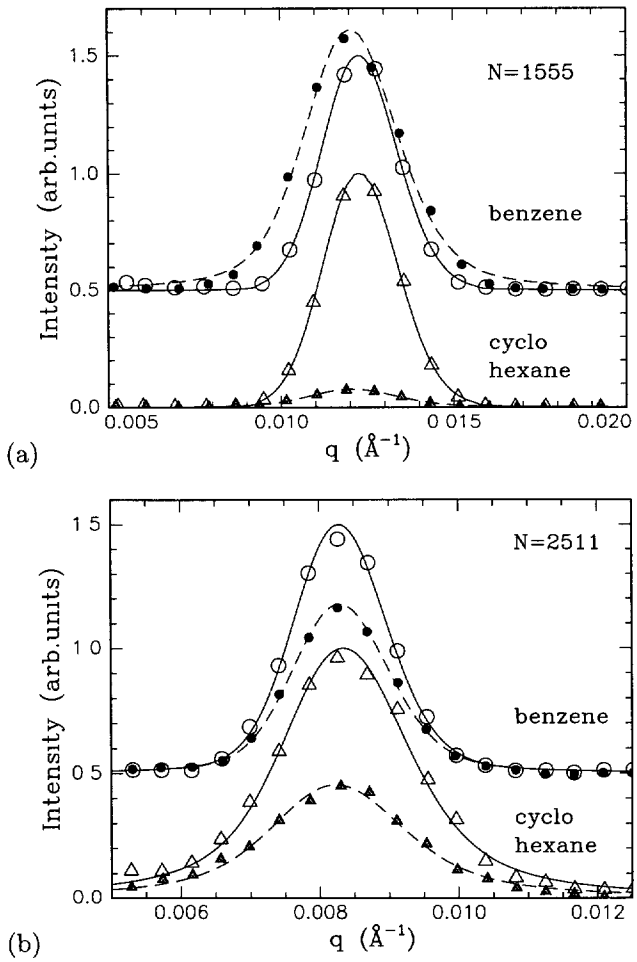

Fig. 10. — Azimuthally averaged and background-corrected SANS spectra from two samples solvent-cast from benzene (circles) and from cyclohexane (triangles), measured at 150 °C. Open symbols: q_y-direction, filled symbols: q_x-direction. The error bars are smaller than the symbol size. The lines are fits of smeared Lorentz-functions to q_y-data (full lines) and to q_x-data (broken lines). (a) The sample solvent-cast from benzene is close to isotropic.

selective solvent for polybutadiene. Azimuthally averaged SANS spectra from these samples together with spectra from samples solvent-cast from benzene are shown in Figure 10. The peak positions as obtained in SAXS and SANS experiments are given in Table III. The differences in q_y^* in spectra from samples solvent-cast from benzene and from cyclohexane are smaller than 3% and are thus negligible.

3.7. Scaling Behavior of the Characteristic Length. — Plotting the peak positions from annealed, solvent-cast (from benzene) and shear aligned samples together (Fig. 11 and Tab. II), no significant differences are observed for the peak positions, *i.e.* the preparation methods used lead to thermal equilibrium.

We also include data from disordered samples in Figure 11. The spectra from these samples show broad peaks (Fig. 12). Spectra obtained with the Kratky-camera were desmeared for

Table III. — *Peak positions of samples solvent-cast from benzene and from cyclohexane; q_y in $10^{-2}Å^{-1}$ ([a]) Kratky-camera, ([b]) SANS.*

sample	N	benzene	cyclohexane
SB06	1555	1.19 ± 0.02^a	1.15 ± 0.02^a
		1.23 ± 0.04^b	1.23 ± 0.04^b
SB07	2511	0.832 ± 0.022^b	0.838 ± 0.022^b

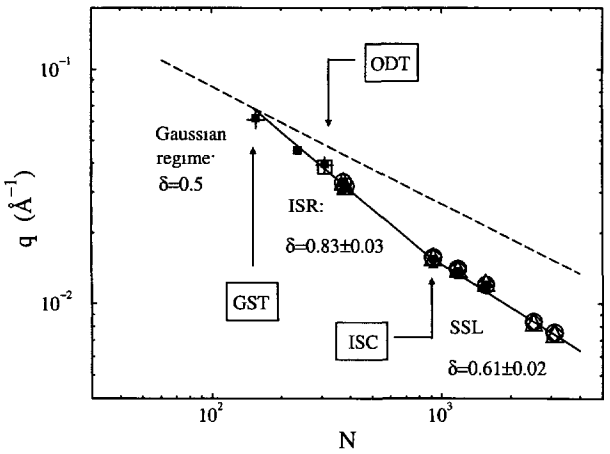

Fig. 11. — Peak positions, q^*, *versus* chain length, N, at 150 °C in a log-log-representation. Squares: disordered samples, circles: annealed samples, triangles: solvent-cast samples, diamonds: shear aligned samples. Open symbols: SANS, filled symbols: Kratky-camera, crosses: pinhole SAXS camera. Full lines: weighted linear fits in the range $N = 156 - 921$ and $N = 921 - 3090$. The dashed line has a slope of -0.5. ISR stands for intermediate-segregation regime, SSL for strong-segregation limit, GST for Gaussian-to-stretched-coil transition, ODT for order-disorder transition and ISC for intermediate-to-strong-segregation crossover.

the beam length as well as for the width effect (Fig. 12). For two samples, the peak positions thus found are reproduced with instruments having pinhole geometry, *i.e.* the procedure for desmearing spectra measured with the Kratky-camera leads to reliable results for the peak positions (Tab. II). A theoretical expression for the peak shape in the disordered state has been given by Leibler [2], but in the present study, Lorentz-functions are fitted to these spectra in order to maintain consistency with the treatment of spectra from ordered samples. Only the positions of the peaks in spectra from disordered samples are used for further analysis. A characteristic length in the disordered state is defined as $D = 2\pi/q^*$, q^* being the peak position.

In order to establish the dependence of the characteristic length on chain length, the peak positions from all three instruments were used. For details of the analysis see reference [8]. Scaling behavior could be assigned within the whole N-range studied, but with a significant change in exponent for small and large values of N: $D \propto N^{0.83\pm0.03}$ for $N = 156 - 921$ and $D \propto N^{0.61\pm0.02}$ for $N = 921 - 3090$. The crossover between these two regimes is located at $N = 905$, which corresponds to $\chi N \simeq 29$. The former region is identified as the Intermediate

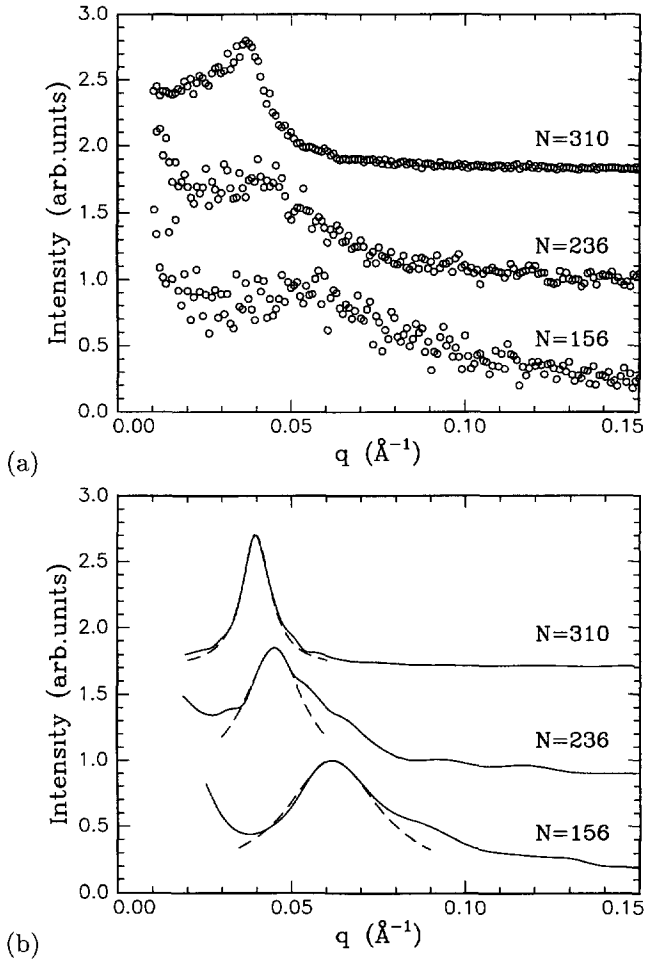

Fig. 12. — (a) Background-corrected SAXS spectra from disordered samples measured at 150 °C using the Kratky-camera. The spectra are shifted vertically by arbitrary amounts. (b) Corresponding desmeared spectra (full lines) together with fits of Lorentz-functions to the peaks (dashed lines). The spectra are shifted vertically.

Segregation Regime (ISR) and the latter one as the SSL. In the following, we discuss the characteristics of the SSL, the crossover to the ISR (the ISC, Intermediate-to-Strong-segregation Crossover) and the characteristics of the ISR.

A characteristic feature of the SSL is that the interphases between the domains are narrow. The SAXS spectra from samples having $N > N_{\mathrm{ISC}}$ display a relatively high number of Bragg-reflections (up to seventh order, Fig. 8). Thus, the narrow-interphase assumption of the SSL-theories is met with these samples. The exponent found in the present work ($\delta = 0.61 \pm 0.02$) is lower than the values predicted for the SSL [5–7]. Nevertheless, we consider the region $N > N_{\mathrm{ISC}}$ as the SSL.

The crossover from the SSL to a scaling regime with higher exponent is observed at $(\chi N)_{\mathrm{ISC}} \simeq 29$, a value which is reasonable compared to the range of predicted values [10–15].

For $\chi N < (\chi N)_{\mathrm{ISC}}$, we observe that the characteristic length scales with chain length like $D \propto N^{0.83 \pm 0.03}$ This value of the exponent is consistent with the values identified with other, chemically different polymers: $\delta = 0.80 \pm 0.04$ with annealed poly(ethylene propylene)-poly(ethylethylene) [16] and $\delta = 0.79 \pm 0.02$ with shear aligned polystyrene-polyisoprene samples [18]. This might indicate that δ is universally close to 0.8 in this regime, depending only weakly on molecular details such as the conformational asymmetry. However, other studies find different values of the exponent [21–23]. The samples used in these studies were solvent-cast below the highest glass temperature of the block copolymers. In this case, one cannot exclude the appearance of non-equilibrium structures. In the present study, the SAXS spectra from ordered samples in the ISR display only one peak, indicating that the concentration profile is close to sinusoidal, in consistency with theories [9–11, 15].

We observe that the ISR reaches into the disordered state, the GST thus being located in the disordered state. This is in consistency with fluctuation theories [19, 20] which predict deviations from Gaussian scaling due to chain stretching already in the disordered state. However, the location of the GST is predicted to depend on the chain length: the larger N, the closer $(\chi N)_{\mathrm{GST}}$ is to $(\chi N)_{\mathrm{ODT}}$. In experimental systems, studies of the N-dependence of the GST are difficult to realize. One is limited by the range of chain lengths which can be synthesized ($N \simeq 20 - 10\,000$). Very short chains, however, are not suitable for studies of the scaling behavior of the characteristic length scale because they are not Gaussian. Very high molar mass polymers, on the other hand, become difficult to handle and thermal equilibrium is difficult to achieve because of the low chain mobilities.

As discussed in references [8, 17], we have identified the lower limit of the ISR in our system using dynamic light scattering to be located at $\chi N \simeq 5$. A line with slope $-1/2$ has therefore been included in Figure 11 for $\chi N < 5$. The degree of chain stretching is related to the distance between the obtained peak position, q^*, and the one expected for Gaussian chains (the dashed line in Fig. 11). The samples having $\chi N > 5$ thus display stretched chain configurations, including the disordered ones. The exponent δ is a measure for how strongly the degree of stretching increases upon increasing the chain length (and thereby χN). From Figure 11, it becomes clear that the deviation from Gaussian scaling with increasing chain length is stronger in the ISR ($\delta = 0.83 \pm 0.03$) than in the SSL ($\delta = 0.61 \pm 0.02$).

No change of scaling behavior is observed at the ODT. This may be related to the fact that the variation of the characteristic length is related to the local shape of the concentration profile, which is only weakly coupled to the appearance of long-range order at the ODT. This finding is consistent with the observations made in a temperature scan with a low molar mass SB sample, discussed in the next section.

3.8. Temperature Behavior at the ODT. — Varying the temperature for a given sample allows more detailed studies in a small χN-range. In order to study the behavior of the characteristic length at the ODT, we measured the temperature behavior of a sample having an accessible ODT temperature (T_{ODT}).

Using SANS, the structure of a low molar mass sample ($N = 310$) having $T_{\mathrm{ODT}} = 130 \pm 2$ °C was studied as a function of temperature between 114 and 150 °C, corresponding to χN in the range 10.1-11.7. Before the measurements, the sample was heated above T_{ODT} and was slowly cooled down to 114 °C.

Upon heating above T_{ODT}, the first-order Debye-Scherrer ring on the two-dimensional detector broadens. The azimuthally averaged spectra are shown in Figure 13 for representative temperatures. Fitting smeared Lorentz-functions to the peak region ($0.025 - 0.055$ Å^{-1}), the peak height, width and position are obtained (Figs. 14 and 15).

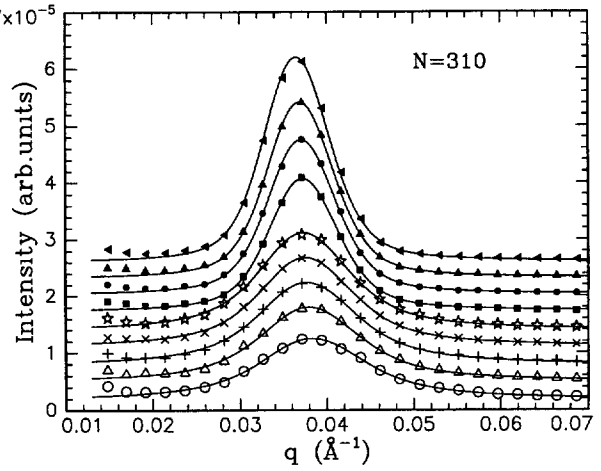

Fig. 13. — Azimuthally averaged and background-corrected SANS spectra from sample SB11 at some representative temperatures. From top to bottom: 114, 122, 126, 129, 130, 134, 138, 142, and 150 °C. The lines are fits of smeared Lorentz-curves. The curves are shifted by 0.3×10^{-5} arb. units.

The peak height and the correlation length, ξ, drop discontinuously between 129 and 130 °C to approximately half their value. This temperature coincides with the ODT temperature determined in the dynamic mechanical experiment (Fig. 1). The discontinuity in peak shape is consistent with the observations made in references [37, 38] and indicates the first-order nature of the phase transition. The integrated intensity, however, which is calculated by integrating over the unsmeared Lorentz-functions (Fig. 14c), decreases upon heating, which is attributed to a gradual decrease of contrast. At T_{ODT}, no significant discontinuity is observed, only a change of slope: In the range 114-126 °C, the slope is $(-0.66 \pm 0.04) \times 10^{-8}$ *arb.units* Å^{-1}/K, whereas a value of $(-0.37 \pm 0.04) \times 10^{-8}$ *arb.units* Å^{-1}/K is obtained in the range 134-150 °C. In the ordered state, the slope is thus a factor 1.8 larger than in the disordered state. The lack of a discontinuity is attributed to the fact that, locally, the concentration profile is very similar just below and just above T_{ODT}, *i.e.* only the long-range organization changes at the ODT.

The peak position, q^*, rises with temperature (Fig. 15) which means that the characteristic length decreases upon heating. This is attributed to an increase in chain flexibility upon heating, resulting in a decrease of the radius of gyration. Lines have been fitted above and below T_{ODT}. In the ordered state (114-126°C), a slope $\mathrm{d}\ln(q^*)/\mathrm{d}T = (0.132 \pm 0.005) \times 10^{-2}$ K^{-1} is obtained, which is identical to the slope in the disordered range (134-150°C): $(0.132 \pm 0.004) \times 10^{-2}$ K^{-1}. However, in a narrow range around T_{ODT} (128-132°C), a higher value is found: $\sim 0.17 \times 10^{-2}$ K^{-1} The finding of a higher slope near the ODT is in consistency with the observations made in references [38–40].

Extrapolating the lines fitted in the ordered and the disordered state to T_{ODT}, a difference in q^* of 4×10^{-5} Å^{-1} is found, which corresponds to a relative discontinuity of the peak position at T_{ODT} of 0.1%. The fact that the discontinuity is so small differs from the observations made by other groups: some groups have observed changes of the peak position at T_{ODT} of several percent [38–40], whereas others have not observed any discontinuous change [37, 41]. The magnitude of the discontinuity of the peak position at T_{ODT} thus seems to depend on the molecular details.

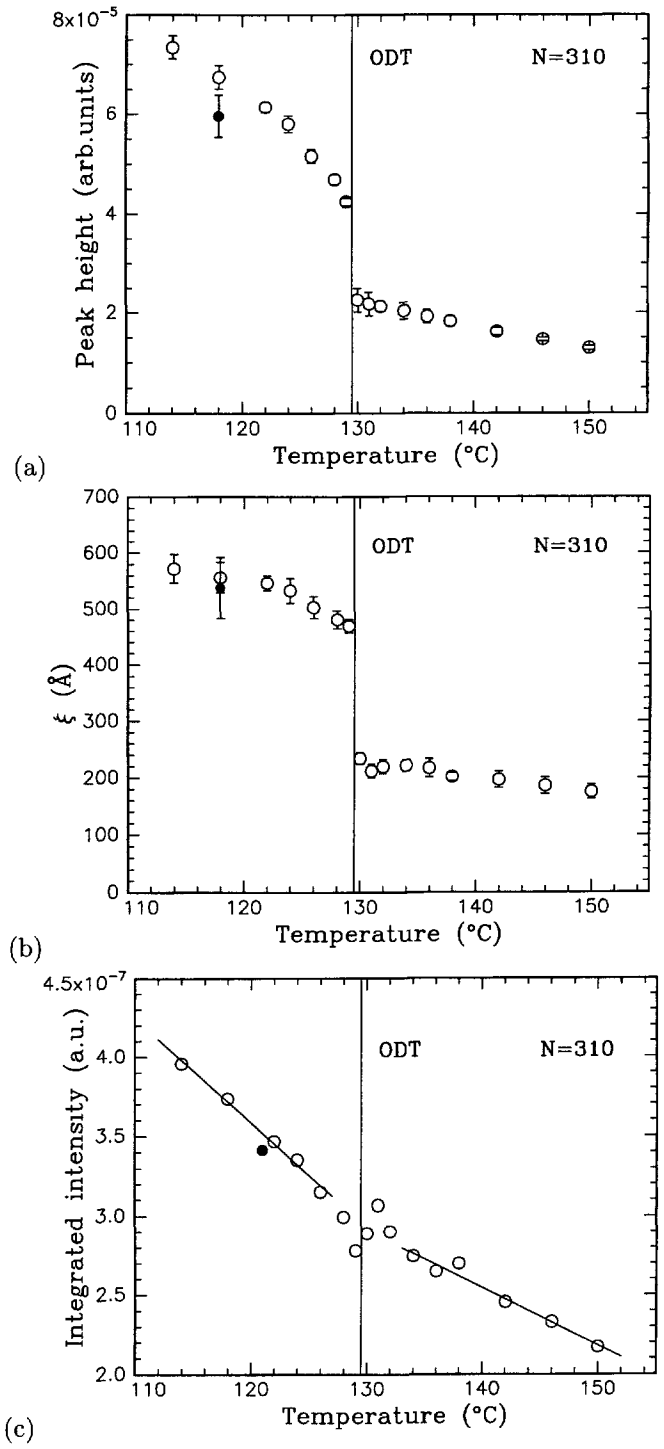

Fig. 14. — Results from the fits to the spectra from sample SB11. (o) Heating run, (•) cooling run. The vertical line indicates the ODT temperature as determined from the drop in peak height (129.5 °C). (a) Peak height I_o *versus* temperature, (b) correlation length ξ *versus* temperature, (c) integrated peak intensity *versus* temperature. The lines are linear fits in the range 114-126 and 134-150 °C to the data from the heating run.

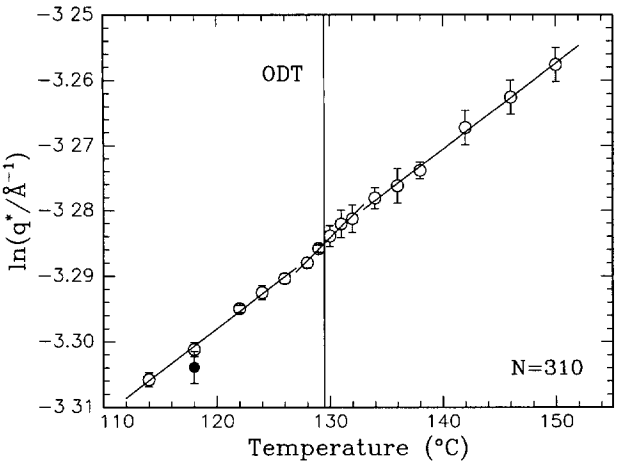

Fig. 15. — Peak positions, q^*, *versus* temperature in a semi-logarithmic plot as obtained with sample SB11. The vertical line indicates the ODT temperature as determined from the drop in peak height (129.5 °C). Lines are linear fits to the temperature regions 114 – 126°C, 128 – 132°C, and 134 – 150°C (heating run).

All values of $\mathrm{d}\ln(q^*)/\mathrm{d}T$ are higher than expected for Gaussian chains. The latter can be calculated applying the definition for the coil expansivity, κ (*e.g.* [42]) to the block copolymer:

$$\kappa_{\mathrm{SB}} = \frac{\mathrm{d}\ln\langle R^2\rangle_0^{\mathrm{SB}}}{\mathrm{d}T} \tag{9}$$

which is equivalent to

$$\ln(q^*) = \mathrm{const} - \frac{\kappa_{\mathrm{SB}}}{2} T \tag{10}$$

assuming $q^* \propto (\langle R^2\rangle_0^{\mathrm{SB}})^{-1/2}$ $\langle R^2\rangle_0^{\mathrm{SB}}$ denotes the unperturbed mean-square end-to-end distance of the SB block copolymer, which for Gaussian chains is given by the sum of the mean-square end-to-end distances of the polybutadiene and the polystyrene block:

$$\langle R^2\rangle_0^{\mathrm{SB}} = \langle R^2\rangle_0^{\mathrm{PS}} + \langle R^2\rangle_0^{\mathrm{PB}} \tag{11}$$

Thus,

$$\kappa_{\mathrm{SB}} = \frac{\langle R^2\rangle_0^{\mathrm{PS}}\,\kappa_{\mathrm{PS}} + \langle R^2\rangle_0^{\mathrm{PB}}\,\kappa_{\mathrm{PB}}}{\langle R^2\rangle_0^{\mathrm{PS}} + \langle R^2\rangle_0^{\mathrm{PB}}}. \tag{12}$$

Using the values for $\langle R^2\rangle_0^{\mathrm{PS}}/M_{\mathrm{PS}}$ and $\langle R^2\rangle_0^{\mathrm{PB}}/M_{\mathrm{PB}}$ given in Section 3.2 together with the molar masses of the two blocks, $M_{\mathrm{PS}} = 9930$ g/mol and $M_{\mathrm{PB}} = 8370$ g/mol and $\kappa_{\mathrm{PS}} = -1.1 \times 10^{-3}\mathrm{K}^{-1}$ [43] and $\kappa_{\mathrm{PB}} = 0$ [26], we find $\mathrm{d}\ln(q^*)/\mathrm{d}T = -\kappa_{\mathrm{SB}}/2 = 2.0 \times 10^{-4}\mathrm{K}^{-1}$ The slopes identified in the present study are a factor 7 and 9 higher. We therefore conclude that the chains are stretched throughout the regime studied. This is in accordance with the observation that the exponent δ is higher than 0.5 for $N = 156 - 310$ at 150 °C, *i.e.* the chains are stretched for $\chi N > 5$ (Sect. 3.7).

4. Summary and Conclusion

In the present study, the bulk structure of a homologous series of symmetric polystyrene-polybutadiene diblock copolymers has been investigated.

Different sample preparation methods have been applied in order to ensure thermal equilibrium. The overall structures obtained differ strongly from each other, however, the values of the lamellar thickness obtained are equal within a few percent. We have analyzed the SANS and SAXS spectra with the aid of simple model calculations of the scattering from lamellar structures.

Annealed samples are found to consist of randomly oriented, lamellar domains, whereas solvent-cast and shear aligned samples are macroscopically oriented to a certain degree. In solvent-cast samples, the lamellar interfaces are parallel to the film surfaces and in shear aligned samples perpendicular to the shear gradient. It is found that, under the present conditions, the shear aligned samples are oriented to a higher degree than the solvent-cast samples.

In solvent-cast and shear aligned samples, the number of correlated lamellae is higher in oriented than in non-oriented domains. For samples prepared in either way, the number of correlated lamellae is maximum for medium molar masses. Close to the ODT, defects of the lamellar structure together with a distribution of lamellar thicknesses might be at the origin of the small number of correlated lamellae. In the SSL, the chain mobilities are so low that the formation of domains is a very slow process.

The concentration profile is shown to be close to sinusoidal in the vicinity of the ODT. It gradually becomes rectangular, *i.e.* the lamellar interfaces become narrower, the deeper the samples are in the ordered state, in accordance with theories.

The scaling behavior of the characteristic length with chain length has been studied using data from samples having chain lengths between 156 and 3090 and being prepared as described above. At a temperature of 150 °C, a χN-range between ~ 5 in the disordered state and ~ 100 deep in the ordered state is investigated. A crossover from an intermediate-segregation regime to the SSL has been identified at $\chi N \simeq 29$. The ISR is characterized by a scaling behavior of the characteristic length $D \propto N^{0\,83\pm0\,03}$, whereas the exponent is 0.61 ± 0.02 in the SSL. No change of scaling behavior is observed at the ODT.

In a temperature scan with a low molar mass sample in the vicinity of T_{ODT}, it is found that the variation of the peak position with temperature is slightly stronger in a narrow region around T_{ODT} than deeper in the disordered and the ordered state. The discontinuity of q^* at T_{ODT}, however, is less than 0.1%. Above and below T_{ODT}, the temperature behavior of q^* is very similar. We therefore do not believe there is experimental evidence for splitting the ISR up into a region located in the disordered state, $(\chi N)_{\mathrm{GST}} < \chi N < (\chi N)_{\mathrm{ODT}}$, and a region located in the ordered state, $(\chi N)_{\mathrm{ODT}} < \chi N < (\chi N)_{\mathrm{ISC}}$. The integrated peak intensity does not change discontinuously at T_{ODT}, which indicates that, locally, the concentration profile is very similar in the disordered and the ordered state close to the ODT. However, both the peak height and width change discontinuously at T_{ODT}, reflecting the first-order nature of the transition.

In summary, the picture emerging includes three regimes: the Gaussian regime at $\chi N < 5-6$ where $D \propto N^{0.49}$ [16,17], the ISR at $\chi N \simeq 5-29$, where $D \propto N^{0\,83}$, and the SSL at $\chi N > 29$, where $D \propto N^{0\,61}$ The Gaussian regime and the SSL are thus linked by a distinct regime, the ISR.

Acknowledgments

We thank T. Zemb, D. Gazeau and L. Arleth for their help with the SAXS measurements at the CEA, Saclay and L. Nielsen, L. Hubert and A.B. Nielsen, Risø National Laboratory for their help with the sample characterization and preparation.

Appendix A

We derive here a way of determining the number of correlated lamellae from the width of the first-order Bragg peak, following standard methods [35].

Consider a single-crystal consisting of a stack of N_s lamellae, the lamellae normal being parallel to the z-direction. In the x- and y-direction, the scattering length (or electron) density is assumed to be constant, *i.e.* the model is one-dimensional. The scattering length density of a lamellar stack is given by the convolution product of the scattering length density of a single lamella, $\rho_s(z)$, and the lattice peak function, $\rho_l(z)$ [35]:

$$\rho_l(z) = \sum_{n=0}^{N_s-1} \delta(z - nD). \tag{A.1}$$

D is the lamellar thickness and $0 \leq n \leq N_s - 1$ is an integer, counting the layers in the stack. The height of the lamellar stack is thus N_sD. The formfactor, $F(q)$, related to the profile of a single lamella, $\rho_s(z)$, is defined by

$$|F(q)|^2 = \left| \int_0^D \mathrm{d}z\, \rho_s(z) \exp(iqz) \right|^2 \tag{A.2}$$

$q = (4\pi/\lambda)\sin(\theta/2)$ is the scattering vector, being parallel to q_z, λ denotes the wavelength and θ the scattering angle. The structure factor related to the lattice peak function is defined by

$$S(q) = \left| \int_0^{N_sD} \mathrm{d}z\, \rho_l(z) \exp(iqz) \right|^2 = \frac{\sin^2(qDN_s/2)}{\sin^2(qD/2)}. \tag{A.3}$$

$S(q)$ has maxima at $q = q_k = 2\pi k/D$, k being an integer. The intensity scattered from a regular stack of lamellae is given by

$$I(q) = |F(q)|^2 S(q). \tag{A.4}$$

Here, the intensity has been normalized.

In the following, two cases are considered: a rectangular and a sinusoidal profile of one block, corresponding to the profiles deep in the ordered state [21] and close to the ODT [44], respectively.

In case of a symmetric rectangular lamellar profile, $\rho_s(z)$ has the form

$$\rho_s(z) = \begin{cases} \Delta\rho & \text{if} \quad 0 < z < D/2, \\ 0 & \text{if} \quad D/2 < z < D. \end{cases} \tag{A.5}$$

Here, $\rho_s(z)$ is measured relative to the density of the pure domain of one block. In this case, the formfactor is given by

$$|F(q)|^2 = \frac{4(\Delta\rho)^2}{q^2} \sin^2\left(\frac{qD}{4}\right). \tag{A.6}$$

The even-order Bragg-reflections (k even) are suppressed by the formfactor, *i.e.* only the odd-order reflections are non-vanishing. As the envelope of $I(q)$ is inversely proportional to q^2, the peak height decreases strongly with increasing order of the reflection.

A sinusoidal profile is described by the expression

$$\rho_s(z) = \frac{\Delta\rho}{2}\left[1 + \sin\left(2\pi\frac{z}{D}\right)\right] \tag{A.7}$$

leading to

$$|F(q)|^2 = (\Delta\rho)^2\left[\frac{1}{q^2} + \left(\frac{2\pi/D}{(2\pi/D)^2 - q^2}\right)^2\right]\sin^2\left(\frac{qD}{2}\right). \tag{A.8}$$

All reflections except the first order are suppressed. The concentration profiles encountered in lamellar block copolymer systems are expected to change from close to sinusoidal near the ODT to close to rectangular in the SSL. This change in concentration profile corresponds to a decrease of the width of the lamellar interfaces. The shape of the concentration profile is reflected in the number of non-vanishing reflections: the more non-vanishing reflections observed, the closer is the concentration profile to rectangular, and the more narrow are the lamellar interfaces.

The width of the first-order Bragg-reflection (centered around $q = 2\pi/D$) depends only weakly on the shape of the profile, but it depends strongly on N_s. Thus, from the width of the first-order Bragg-reflection, the number of correlated lamellae, N_s, can be estimated, provided that the distribution of lamellar thicknesses is narrow. Defining the half width at half maximum, q_H, by

$$I\left(\frac{2\pi}{D} + q_H\right) = \frac{1}{2}I\left(\frac{2\pi}{D}\right) \tag{A.9}$$

the following condition for q_H is found for a rectangular profile, using equations (A.3, A.4 and A.6):

$$\left[\frac{\pi/N_s}{q_H D + 2\pi}\frac{\sin(q_H D N_s/2)}{\sin(q_H D/4)}\right]^2 = \frac{1}{2}. \tag{A.10}$$

This equation is solved by $q_H = c/(N_s D)$ where c is weakly N_s-dependent: c increases with N_s from 2.49 for $N_s = 5$ to 2.77 for $N_s = 100$. For the first-order Bragg-reflection of a sinusoidal profile (Eqs. (A.3, A.4 and A.8)), the condition

$$\left(\frac{4}{DN_s}\right)^2\left[\frac{1}{(2\pi/D + q_H)^2} + \left(\frac{2\pi/D}{q_H(4\pi/D + q_H)}\right)^2\right]\sin^2\left(\frac{q_H D N_s}{2}\right) = \frac{1}{2} \tag{A.11}$$

leads to values for c between 2.67 and 2.78. In the following, $c = 2.75$ is used in both cases. With this value, the error in the determination of N_s is smaller than 10%.

References

[1] Bates F.S. and Fredrickson G.H., *Annu. Rev. Phys. Chem.* **41** (1990) 525.
[2] Leibler L., *Macromol.* **13** (1980) 1602.
[3] Fredrickson G.H. and Helfand E., *J. Chem. Phys.* **87** (1987) 697.
[4] Bates F.S., Schulz M.F., Khandpur A.K., Förster S., Rosedale J.H., Almdal K. and Mortensen K., *Faraday Discuss.* **98** (1994) 7.
[5] Helfand E. and Wasserman Z.R., *Macromol.* **9** (1976) 879.
[6] Semenov A.N., *Sov. Phys. JETP* **61** (1985) 733. (*Zh. Eksp. Teor. Fiz.* **88** (1985) 1242.

[7] Ohta T. and Kawasaki K., *Macromol.* **19** (1986) 2621.
[8] Papadakis C.M., Almdal K., Mortensen K. and Posselt D., *Europhys. Lett.* **36** (1996) 289.
[9] Melenkevitz J. and Muthukumar M., *Macromol.* **24** (1991) 4199.
[10] Shull K.R., *Macromol.* **25** (1992) 2122.
[11] Vavasour J.D. and Whitmore M.D., *Macromol.* **25** (1992) 5477.
[12] Tang H. and Freed K.F., *J. Chem. Phys.* **96** (1992) 8621.
[13] McMullen W.E., *Macromol.* **26** (1993) 1027.
[14] Sones R.A., Terentjev E.M. and Petschek R.G., *Macromol.* **26** (1993) 3344.
[15] Matsen M.W. and Bates F.S., *Macromol.* **29** (1996) 1091.
[16] Almdal K., Rosedale J.H., Bates F.S., Wignall G.D. and Fredrickson G.H., *Phys. Rev. Lett.* **65** (1990) 1112.
[17] Papadakis C.M., Brown W., Johnsen R.M., Posselt D. and Almdal K., *J. Chem. Phys.* **104** (1996) 1611.
[18] Hadziioannou G. and Skoulios A., *Macromol.* **15** (1982) 258.
[19] Olvera de la Cruz M., *Phys. Rev. Lett.* **67** (1991) 85.
[20] Barrat J.-L. and Fredrickson G.H., *J. Chem. Phys.* **95** (1991) 1281.
[21] Hashimoto T., Shibayama M. and Kawai H., *Macromol.* **13** (1980) 1237.
[22] Richards R.W. and Thomason J.L., *Macromol.* **16** (1983) 982.
[23] Matsushita Y., Mori K., Saguchi R., Nakao Y., Noda I. and Nagasawa M., *Macromol.* **23** (1990) 4313.
[24] Ndoni S., Papadakis C.M., Bates F.S. and Almdal K., *Rev. Sci. Instrum.* **66** (1995) 1090.
[25] Polymer Handbook, J. Brandrup and E.H. Immergut. Eds. (Wiley-Interscience, New York, 1975).
[26] Fetters L.J., Lohse D.J., Richter D., Witten T.A. and Zirkel A., *Macromol.* **27** (1994) 4639.
[27] Papadakis C.M., PhD thesis, Roskilde University, Denmark, April 1996.
[28] Papadakis C.M., Almdal K. and Posselt D., *Il Nuovo Cimento* **16D** (1994) 835.
[29] Hadziioannou G., Mathis A. and Skoulios A., *Colloid & Polymer Sci.* **257** (1979) 136.
[30] Pedersen J.S., Posselt D. and Mortensen K., *J. Appl. Cryst.* **23** (1990) 321.
[31] LeFlanchec V., Gazeau D., Taboury J. and Zemb Th., *J. Appl. Cryst.* **29** (1996) 110.
[32] Bates F.S., Rosedale J.H., Bair H.E. and Russell T.P., *Macromol.* **22** (1989) 2557.
[33] Flory P.J., Principles of Polymer Chemistry (Cornell University Press, 1953).
[34] Khandpur A.K., Förster S., Bates F.S., Hamley I.W., Ryan A.J., Bras W., Almdal K. and Mortensen K., *Macromol.* **28** (1995) 8796.
[35] Hosemann R. and Bagchi S.N., Direct analysis of diffraction by matter (North-Holland Publishing Company, 1962).
[36] Glatter O. and Gruber K., *J. Appl. Cryst.* **26** (1993) 512.
[37] Bates F.S., Rosedale J.H. and Fredrickson G.H., *J. Chem. Phys.* **92** (1990) 6255.
[38] Stühn B., Mutter R. and Albrecht T., *Europhys. Lett.* **18** (1992) 427.
[39] Bartels V.T., Abetz V., Mortensen K. and Stamm M., *Europhys. Lett.* **27** (1994) 371.
[40] Rosedale J.H., Bates F.S., Almdal K., Mortensen K. and Wignall G.D., *Macromol.* **28** (1995) 1429.
[41] Sakamoto N. and Hashimoto T., *Macromol.* **28** (1995) 6825.
[42] Mark J.E. and Flory P.J., *J. Am. Chem. Soc.* **86** (1964) 138.
[43] Mays J.W., Hadjichristidis N. and Fetters L.J., *Macromol.* **18** (1985) 2231.
[44] Foster M.D., Sikka M., Singh N., Bates F.S., Satija S.K. and Majkrzak C.F., *J. Chem. Phys.* **96** (1992) 8605.